The effect of deposition parameters on radiofrequency sputtered molybdenum thin films

2008 J. Phys.: Condens. Matter 20 055206

(http://iopscience.iop.org/0953-8984/20/5/055206)

J. Phys.: Condens. Matter **20** (2008) 055206 (5pp) doi:10.1088/0953-8984/20/05/055206

The effect of deposition parameters on radiofrequency sputtered molybdenum thin films

H Khatri and S Marsillac

Center for Photovoltaics Innovation and Commercialization, University of Toledo, M.S. 111, Toledo, OH 43606, USA

E-mail: Sylvain.Marsillac@utoledo.edu

Received 28 August 2007, in final form 2 December 2007
Published 14 January 2008
Online at stacks.iop.org/JPhysCM/20/055206

Abstract

Employing r.f. (radiofrequency) magnetron sputtering, molybdenum thin films were fabricated on soda-lime glass substrates for use in Cu(In, Ga)Se_2 based solar cells. The physical, electrical and structural properties of the films were studied as a function of two deposition parameters: argon pressure and r.f. power. The strain reversal from tensile to compressive occurs at high pressure and is found to decrease with increasing applied r.f. power. The grain sizes of films deduced from x-ray diffraction measurements (full width at half-maximum), and consistent with atomic force microscope images, increase with increasing argon pressure and power. The resistivity of the films was found to increase with increasing argon pressure and decrease with increasing r.f. power.

(Some figures in this article are in colour only in the electronic version)

1. Introduction

Molybdenum is currently the most common material used for Cu(In, Ga)Se_2 (CIGS) solar cell back contacts. Several properties are required to fulfill this role, notably chemical and mechanical inertness during the other deposition processes, high conductivity, low resistance contact with the CIGS layer, and commensurate coefficient of thermal expansion [1]. A wide variety of other materials such as W, Ta, Nb, Cr, V, Ti, and Mn have also been investigated without any improvement compared to Mo, and often lower cell efficiency due to chemical reactivity [1]. However, the deposition of a molybdenum film as a back contact is not by itself an assurance of a high efficiency solar cell. The deposition parameters and process play a key role in obtaining a layer with the appropriate properties. Extensive research has been done on the deposition of molybdenum thin films by dc sputtering (e.g. [1–5]). However, as the potential portfolio applications of CIGS expand, different films' properties may be required to adapt to new requirements. In this paper, we therefore used r.f. magnetron sputtering to deposit Mo thin films on soda-lime glass. To our knowledge, little research has been performed on Mo thin films deposited by this method [6–12]. To assess the potential of this process, the mechanical, physical and electrical properties of molybdenum thin films were studied as a function of two parameters: argon pressure and r.f. power.

2. Experiments

Molybdenum (Mo) thin films were deposited on ultrasonically cleaned soda-lime glass (SLG) substrates by a r.f. magnetron sputtering system using high purity Mo targets (99.95%). The thickness was kept constant at 0.5 μm. The substrates were not heated, with a maximum temperature monitored during the sputtering process of 40 °C. The deposition was performed under pure argon gas (99.998%) flowing at 10 sccm. Uniform films thickness (±5% error) was achieved using a rotatable substrate holder (12 rpm) fixed 6 cm away from the target. Two different sets of films were prepared by changing a specific parameter, with the others remaining constant. In one case, the argon pressure was varied between 4 and 20 mTorr, while keeping a constant r.f. power of 100 W. In the other case, the r.f. power applied to the target was varied between 20 and 120 W, while keeping a constant argon pressure of 10 mTorr.

The physical, electrical and structural properties of the films were then characterized. The film resistivity was calculated from the sheet resistance measured by four-point

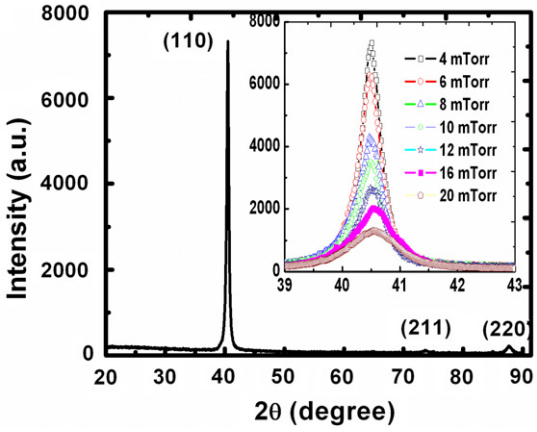

Figure 1. A typical XRD pattern for r.f. sputtered molybdenum thin film (inset: close-up of the (110) peak profiles as a function of argon pressure).

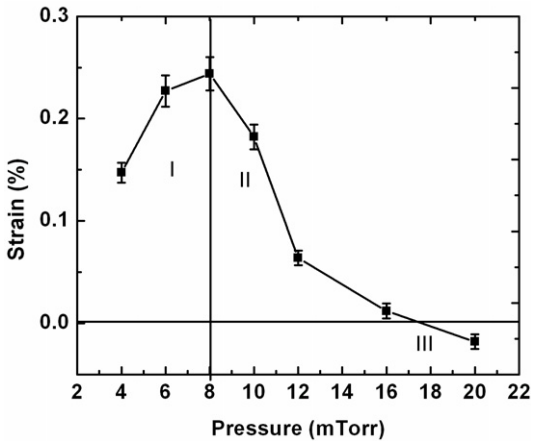

Figure 2. Strain of the r.f. sputtered molybdenum films as a function of argon pressure.

Table 1. XRD, electrical and adhesion measurements as a function of argon pressure for r.f. sputtered molybdenum thin films.

Pressure (mTorr)	Strain (%)	FWHM (deg)	Orientation (110)	Tape test	Resistivity ($\mu\Omega$ cm)
4	0.147	0.37	0.92	Pass	54
9	0.227	0.42	0.89	Pass	78
8	0.244	0.55	0.91	Pass	99
10	0.182	0.53	0.90	Pass	170
12	0.064	0.73	0.89	Pass	280
16	0.012	0.76	0.89	Pass	415
20	−0.018	0.92	0.90	Pass	490

probe and the film thickness measured by DekTak^{3}ST surface profiler. A non-contact AC mode (320 kHz tip) of an atomic force microscope (AFM) was used for the topographical images of the films. The acquired AFM images were used to determine the roughness of the films and the grain sizes and were compared to the results obtained by XRD peak broadening. The influence of process parameters on the crystallographic properties and the mechanical properties of films were studied by x-ray diffraction using a XPERT-PRO diffractometer. The x-ray scans were performed using the Cu Kα (0.154 nm) radiation in a scanning 2θ mode with 0.01° step size. The physical properties, i.e. adhesion of the films to the substrates, were examined using an adhesive scotch tape test. The samples were scratched to a rectangle shape and adhesive tape stripes of same length were glued on the scratched films and stripped with approximately equal amounts of force.

3. Results and discussions

3.1. Study as a function of the argon pressure

3.1.1. X-ray diffraction (XRD). The results of the XRD measurements are summarized in table 1 and a typical spectrum is shown in figure 1. Three main peaks were observed with orientation along the (110), (211) and (220) directions.

The diffraction data were fitted with a Lorentzian function to determine the location of each peak 2θ. Using Bragg's law, the interplanar lattice spacing, $d_{(110)}$, was calculated. The variation of the average lattice spacing, i.e. the slight shift of the (110) peak position, in the direction normal to the plane of the films gives the strain on films; it is either compressive or tensile. The strain on films is calculated using the following formula:

$$\text{Strain}\ (\%) = \frac{\Delta a}{a} \times 100 \qquad (1)$$

where 'a' is the lattice constant (for the molybdenum reference, $a = 0.314\,69$ nm), and the main parameter to determine whether the strain is tensile or compressive. The origin of the strain profiles in the sputtered Mo films may be related to several factors, including voids, oxygen or argon impurities, and crystallographic flaws [13]. The high strain on the films can cause adhesion problems and compromise long term reliability. Most of our films were in tensile strain (figure 2). Starting from low pressure, the strain increases first with increasing pressure and reaches a maximum value at 8 mTorr (region I); it then decreases with further increase in pressure (region II) until it goes into a compressive strain around 17 mTorr (region III). In region I, the decrease in tensile strain with decreasing pressure is attributed to the less frequent formation of voids resulting from the impact of higher energetic particles at low pressures. At low enough pressure, one can see that the films would probably also reach a compressive strain (the limit in our case is due to the design of the deposition chamber). In region II, the increase of pressure increases the frequency of gas phase collisions, reducing the kinetic energy of sputtered neutral atoms and reflected neutrals bombarding the growing films. The decrease in tensile strain with decreasing incident kinetic energy (i.e., increasing working gas pressure) may be due to a microstructural change from a densely packed network with atomic scale voids to a micro-columnar structure, associated with the incorporation of impurities such as O, H [14–16]. In region III, the decrease in tensile strain is high enough and induces a compressive strain.

The degree of orientation of the films along the (110) direction, $P(110)$, was calculated by:

$$P(110) = \frac{I(110)}{I_0(110)} + \frac{I(220)}{I_0(220)} \Big/ \sum_{hkl} \frac{I(hkl)}{I_0(hkl)} \qquad (2)$$

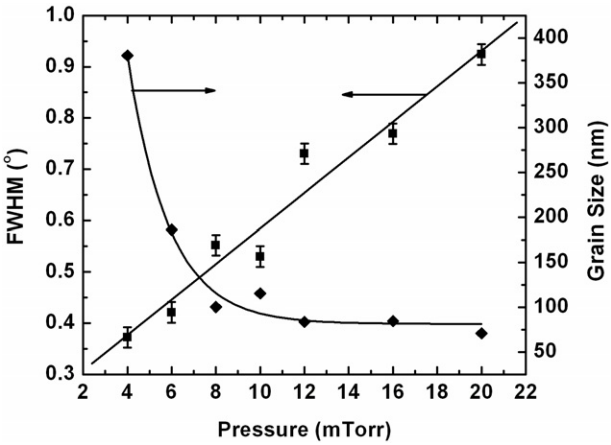

Figure 3. FWHM and grain size of the r.f. sputtered molybdenum thin films as a function of argon pressure. The curves are a guide to the eye.

where $I(hkl)$ is the measured intensity of the peak (h, k, l) for the film and $I_0(hkl)$ the relative powder intensity. The results are reported table 1. It was found that all the Mo films crystallized in the body-centered cubic $Im3m$ phase and that the crystallites were oriented along the (110) plane, which is typical for Mo films deposited at room temperatures. For a bcc lattice material such as Mo, the (110) planes have effectively the highest planar packing density and a minimum surface free energy.

The variation of the full width at half-maximum (FWHM) for the (110) peak as a function of the deposition pressure is reported in table 1 and figure 3. The average particle size of the molybdenum films can be calculated from the broadening of the corresponding (110) x-ray peaks using Scherrer formula [17]:

$$L = K\lambda/\beta\cos(\theta) \tag{3}$$

where L is the crystallite size, K is the Scherrer constant (0.90 in our case), λ is the wavelength of the x-ray, β is the real width of the peak ($\beta^2 = B^2 - b^2$ where B = experimental width, b = instrumental resolution) and θ is the Bragg angle. The crystallite size was found to decrease from 380 to 70 nm as the pressure increases, with a proportional trend obviously for the FWHM.

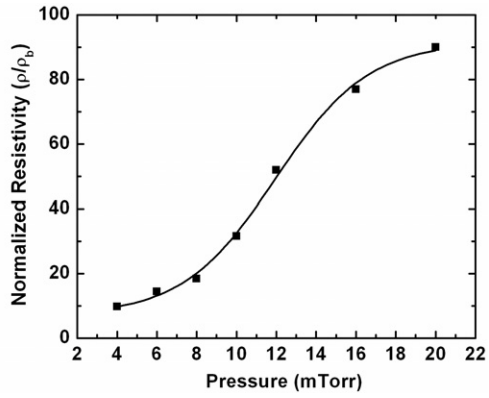

Figure 5. Normalized resistivity of the r.f. sputtered molybdenum thin films as a function of argon pressure.

3.1.2. Atomic force microscopy (AFM). Figure 4 displays an AFM surface topography showing the particle size of the molybdenum films on the glass substrate. AFM studies showed good agreement with XRD measurements: the films deposited at higher pressures were rougher and with smaller grain size compared to the films deposited at low pressures. The average RMS roughness increased from 3.6 to 10.0 nm at higher pressures.

3.1.3. Electrical measurements and mechanical test. The resistivity of the films was calculated by multiplying the sheet resistance and the thickness of the films. The sheet resistance was measured by four-point probe and the thickness by Dektak^{3}ST surface profiler. The values of the resistivity as a function of pressure are reported in table 1. The normalized resistivities of the films (resistivity of the film divided by the resistivity of the molybdenum bulk (5.4 $\mu\Omega$ cm at room temperature)) are plotted in figure 5, as a function of the argon pressures. Films with higher resistivity were obtained at higher pressures, which can be explained by the smaller size of the grains and the higher concentrations of the oxygen present in the films. It is interesting to note that higher efficiency CIGS solar cells are obtained in the presence of sodium (Na), which is often provided by the glass itself through the molybdenum back contact [2]. The presence of oxygen in the molybdenum might play a role in this process, and should therefore not be

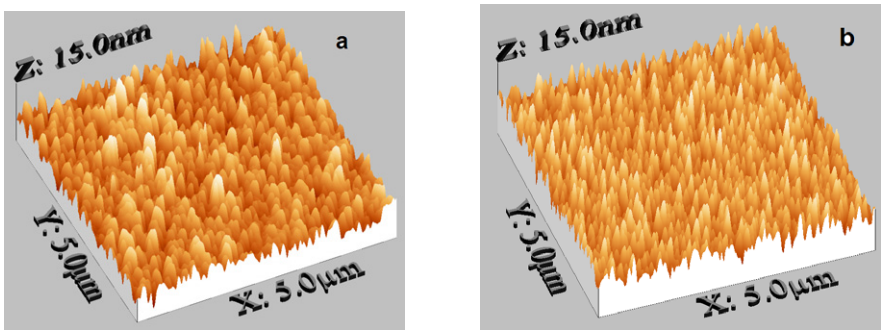

Figure 4. Differences in grain size and morphology of the r.f. sputtered molybdenum thin films at different argon pressures as revealed by AFM top surfaces images (5 μm $\times$ 5 μm). (a) 4 mTorr and (b) 20 mTorr.

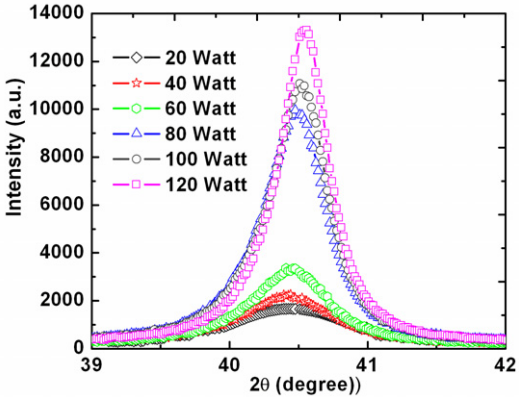

Figure 6. XRD (110) peaks of the r.f. sputtered molybdenum thin films deposited as a function of target power.

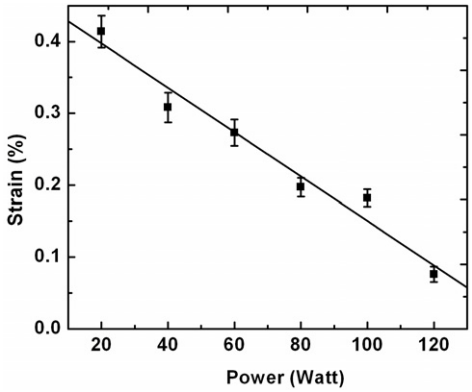

Figure 7. Strain of the r.f. sputtered molybdenum thin films deposited as a function of target power.

Table 2. XRD, electrical and adhesion measurements as a function of target power for r.f. sputtered molybdenum thin films.

Power (W)	Strain (%)	FWHM (deg)	Orientation (110)	Tape test	Resistivity ($\mu\Omega$ cm)
20	0.414	1.22	0.77	Pass	1500
40	0.308	0.80	0.86	Pass	867
60	0.273	0.62	0.92	Pass	278
80	0.197	0.58	0.91	Pass	211
100	0.182	0.53	0.91	Pass	170
120	0.076	0.42	0.96	Pass	72

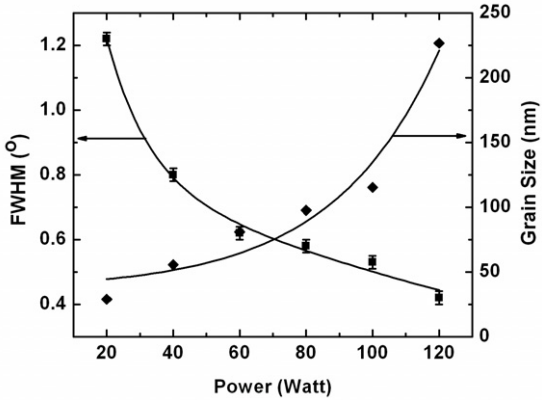

Figure 8. FWHM and grain size of the r.f. sputtered molybdenum thin films as a function of target power. The curves are a guide to the eye.

regarded as necessarily detrimental to the solar cell fabrication process.

The adhesion of the film to the substrate was studied by simple adhesive scotch tape test. The samples were scratched in a rectangle and the adhesive tape stripes of same length were glued on the scratched films and stripped with approximately equal amounts of force. All of the films passed the adhesion test, which is not the case for equivalent films deposited by dc sputtering [2].

3.2. Study as a function of target power

3.2.1. XRD. The XRD results are summarized in table 2 and the (110) peaks are plotted figure 6 as a function of target power. One can see that the films deposited at high power are crystallized with large grains whereas the films deposited at low power are more randomly oriented and with smaller grains. In the range of applied target powers, all the films grow with a (110) preferential orientation.

The shift of the (110) peak along 2θ allowed us to calculate the strain of the films and is plotted in figure 7. All the films showed tensile strain. This stain may result from the microvoids in the thin films due to attractive interaction of atoms across the voids. The less frequent formation of microvoids at high target powers (i.e. higher growth rates) may results in the decrease of the tensile strain.

The degree of orientation of the films along the (110) direction, $P(110)$, calculated by equation (2) was found to increase from 0.75 to 0.95 at high applied power. The increase in crystallite size from 30 to 226 nm at higher power, calculated using the Scherrer formula, is correlated to the decrease of FWHM (figure 8). It is probable that at higher power the particles tend to nucleate with each other more easily to form larger grain size due to the higher flux.

3.2.2. AFM. The AFM pictures showing the grain sizes and the surface morphology of the films grown on glass substrates are presented figure 9. A reduced surface roughness of the films along with larger crystallites is observed for films deposited with higher applied power, in agreement with the XRD and strain observation.

3.2.3. Electrical measurements and mechanical test. The resistivity of the films as a function of target power are reported in table 2. The normalized resistivities of the films (resistivity of the film divided by the resistivity of the molybdenum bulk (5.4 $\mu\Omega$ cm at room temperature)) as well as the deposition rate are plotted in figure 10 as a function of the target power. As expected, the deposition rate increases linearly with the target power, allowing the good control of the film processing. The resistivity continuously decreases as the target power increases. Similarly to the previous case, the evolution of the conductivity

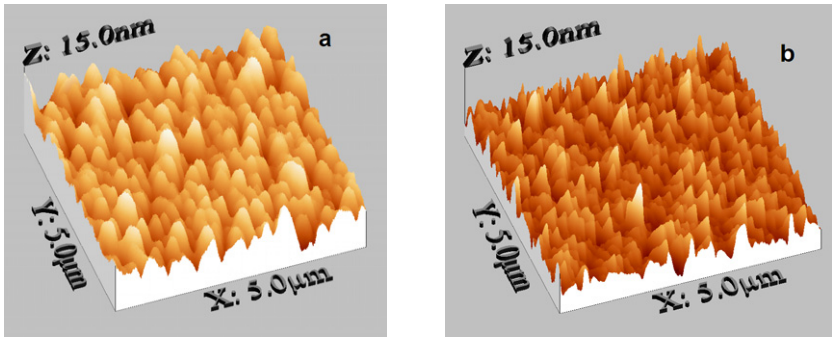

Figure 9. Differences in grain size and morphology of the r.f. sputtered molybdenum thin films at different target powers: (a) 120 W and (b) 20 W.

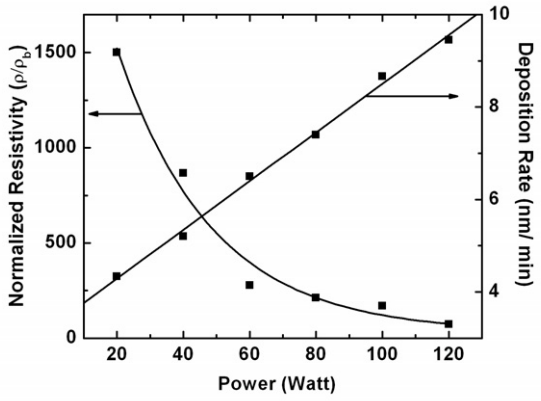

Figure 10. Normalized resistivity and deposition rate of the r.f. sputtered molybdenum thin films as a function of target powers.

is correlated with the evolution of the grain size. It is however important to note that the grain size does not solely determine the electrical properties of the films, which also depend on the grain growth mechanism, and the amounts of voids present on the films and the microstructures as well [16]. The disoriented nature of the films at low target power, correlated to small grain size, also probably contributes to the high resistivity.

The adhesion of the film to the substrate was studied by simple adhesive scotch tape test. Here also, all of the films passed the adhesion test, which is not the case for equivalent films deposited by dc sputtering [2].

4. Conclusions

R.f. magnetron sputtering was used to deposit molybdenum thin films on soda-lime glass. It was found that the working gas pressures and the r.f. target power influence the physical, electrical and structural properties of the films. We obtained low resistivity for films deposited at low argon pressure or high r.f. power. To minimize the back contact contribution to the series resistance in solar cells, one desires indeed low resistive films. Another important parameter for a good back contact is its ability to adhere to the substrate, allowing for durable modules to be fabricated and warranty to be respected. In this study, we have shown that molybdenum thin films deposited by r.f. magnetron sputtering may have better adhesion to the glass than films deposited by dc magnetron sputtering under the same conditions. This result needs to be confirmed by direct comparison, in the same system, between r.f. and dc deposited molybdenum thin films and expanded to the case of flexible substrates, which is an important potential market for CIGS solar cells.

Acknowledgments

The authors would like to thank Drs Deng and Compaan for their help in the film deposition and Dr Collins for his helpful suggestions.

References

[1] Orgass K, Schock H W and Werner J H 2003 *Thin Solid Films* **431–432** 387
[2] Scofield J H, Duda A, Albin D, Ballard B L and Predecki P K 1995 *Thin Solid Films* **260** 26
[3] Kadam A A, Jahagirdhar A H and Dhere N G 2005 *Proc. Material Research Society Symp. (San Francisco)* vol 865 pp 423–9
[4] Al-Thani H A, Hasoon F S, Yang M, Asher S, Alleman J L, Al-Jassim M M and Williamson D L 2002 *Proc. 29th IEEE Photovoltaic Specialist Conf. (New Orleans)* pp 720–3
[5] Gordillo G, Grizalez M and Hernandez L C 1998 *Sol. Energy Mater. Sol. Cells* **51** 327
[6] Tinone M C K, Haga T and Kinoshita H 1996 *J. Electron Spectrosc. Relat. Phenom.* **8** 461
[7] Assmann L, Bernede J C, Drici A, Amory C, Halgand E and Morsli M 2005 *Appl. Surf. Sci.* **246** 159
[8] Miyata N and Akiyoshi S 1985 *Appl. Phys.* **58** 1651
[9] Martinez M A and Guillen C 1998 *Surf. Coat. Technol.* **110** 62
[10] Dicov Ch, Marinov M, Maciel H, Grigorov K, Nedkov I and Beshkov G 2005 *J. Optoelectron. Adv. Mater.* **7** 385
[11] Wada T 1997 *Sol. Energy Mater. Sol. Cells* **49** 249
[12] Nagano J 1980 *Thin Solid Films* **76** 1
[13] Malhotra S G, Rek Z U, Yalisove S M and Bilello J C 1997 *J. Vac. Sci. Technol.* A **15** 345
[14] Yamaguchi T and Miyagawa R 1991 *Japan. J. Appl. Phys.* **30** 2069
[15] Blech I and Cohen U 1982 *J. Appl. Phys.* **53** 4202
[16] Windischmann H, Collins R W and Cavese J M 1986 *J. Non-Cryst. Solids* **85** 261
[17] Kasai N and Kakudo M 2005 *X-ray Diffraction by Macromolecule* (New York: Springer) pp 364–5